A Survey of Temperature Measurements in Convective Clouds

ANDREY A. SINKEVICH

Cloud Seeding and Solar Radiation Studies, Department of Cloud Physics, A. I. Voeikov Main Geophysical Observatory, Saint Petersburg, Russia

R. PAUL LAWSON

SPEC, Inc., Boulder, Colorado

(Manuscript received 19 September 2003, in final form 23 November 2004)

ABSTRACT

A brief review of errors associated with aircraft measurements of temperature in cumulus clouds is presented. This analysis forms the basis for the introduction of a compilation of in-cloud temperature measurements that the authors deem reliable. The measurements are mostly from radiometric thermometers, along with some carefully selected measurements taken with immersion thermometers. The data were collected in cumuli and cumulonimbi in Russia, the United States, and the central Pacific. An estimate of the in-cloud temperature measurement uncertainty is on the order of 0.5°C. The results suggest that the average temperature excess in cumulus clouds, when averaged over the cloud lifetime, is about 0.2°–0.3°C; this value may be biased to an unknown extent, however, by latencies inherent in identification and aircraft sampling of candidate clouds. The maximum temperature excess in growing cumulus congestus is about 2.5°–4°C. In the weak-echo regions of large thunderstorms, the temperature excess is at least 6°–8°C. The average and maximum temperature excesses in cumulus congestus over land are about 0.5°–1°C greater than over the ocean. Measurements of the spatial and vertical distributions of in-cloud temperature excess are presented. Some measurements that pertain to the structure of in-cloud temperature are also discussed.

1. Introduction

Reliable measurements of temperature in cumulus clouds are important for improving our understanding of cloud physics, cloud dynamics, and for validating cloud-resolving models. One example is the effect that entrainment has on cloud buoyancy, lifetime, and precipitation efficiency (Cooper and Lawson 1984; Blyth et al. 1988; Blyth 1993; Wei et al. 1998). Measurement of the source and amount of environmental air entrained into cumulus clouds can be deduced from a technique introduced by Paluch (1979) and requires accurate measurements of temperature in clouds (Lawson and Cooper 1990). Klaassen and Clark (1985) introduced the newest generation of cloud-resolving models, which attempt to incorporate the effects of entrainment and mixing into cumulus simulations. Subsequent enhancements (e.g., Krueger et al. 1997) show some reasonable comparisons with in-cloud profiles of liquid water content. However, in-cloud comparisons with temperature have not been attempted. This may be because of errors associated with typical in-cloud temperature sensors or because of natural variability in environmental temperature due to gravity waves, cloud detrainment, and other factors that create temperature gradients in clear air.

Wei et al. (1998) show that in-cloud temperature excess is the principal component of cloud buoyancy, which is generally positively correlated with vertical velocity in growing tropical convective cells. They conclude that entrainment was a significant factor in reducing buoyancy. Cloud buoyancy also has an interaction on upscale atmospheric processes, such as the vertical transport of mass and momentum in mesoscale systems (LeMone 1983). The National Aeronautics and Space Administration Tropical Rainfall Measuring Mission (TRMM) science team concluded that vertical profiles of precipitation and related profiles of latent heat release produced by tropical convective clouds are needed to understand the Madden–Julian waves that

Corresponding author address: R. Paul Lawson, SPEC, Inc., 3022 Sterling Circle, Suite 200, Boulder, CO 80305.
E-mail: plawson@specinc.com

© 2005 American Meteorological Society

modulate rain in the Tropics. These waves then propagate from the Tropics, affecting global weather features in distant locations (Simpson et al. 1988).

Most airborne temperature measurements have been collected using "immersion thermometers," which employ a sensing element that is immersed into the ambient airstream. Errors associated with immersion thermometry have been known for over 50 years (e.g., Barrett and Reihl 1948; Pinus 1953; Lenschow and Pennell 1974; LeMone and Zipser 1980; Lawson and Cooper 1990). The errors are mostly associated with the uncertainties in quantifying the effect of cloud drops impacting the sensor and/or its housing. Various investigators (e.g., Zaytcev and Ledohovich 1970; Lenschow and Pennell 1974; Lawson and Cooper 1990) have presented theoretical arguments leading to quantification of these errors. The error from sensor wetting is often of the same order (i.e., from one to a few degrees Celsius) as the magnitude of temperature excess/decrease in cumulus clouds (Lawson and Cooper 1990; Wei et al. 1998). Thus, it is necessary to consider immersion temperature measurements carefully on a case-by-case basis and to eliminate those measurements with errors that are a substantial fraction of the cloud property being examined.

Radiometric measurements of temperature in clouds do not suffer from most of the problems associated with sensor wetting that confound immersion temperature sensors (Lawson and Cooper 1990). In this sense, radiometric thermometry can be an inherently improved method for measuring temperature in cumulus clouds. However, radiometers used to measure atmospheric temperature are technically more complex than immersion thermometers, require careful calibration, and are more subject to baseline drift. In this sense, one must take care to scrutinize radiometric temperature measurements to avoid a false interpretation of the results. Also, radiometric temperature measurements inherently have a larger sample volume than measurements from immersion sensors. The larger sample volume can be an advantage because a significant portion of the radiometric sample volume is displaced from the aircraft and away from the influence of the flow distortion caused by the aircraft. On the other hand, the relatively long sample path of radiometric measurements (from about 10 m to kilometers, depending on wavelength) makes it impossible to study finescale fluctuations.

In this paper, we discuss errors in the measurement of in-cloud temperature and present a composite dataset of reliable in-cloud temperature measurements collected in convective clouds at various locations. The data include radiometric measurements and some additional measurements from immersion thermometers that are shown to be sufficiently reliable under certain conditions. The dataset includes airborne measurements of temperature made in cumulus clouds from 1977 to 1993 in northwestern Russia, the United States, the Caribbean Sea, the western Pacific Ocean, and the equatorial Pacific Ocean. Several of the measurements we present were made with radiometric thermometers operating at two wavelengths: a Russian 6.3-μm instrument developed by Sinkevich (1979) and a 4.25-μm device developed by Nelson (1982) and evaluated by Lawson and Cooper (1990).

There are two primary objectives of this paper. The first goal is to discuss errors associated with in-cloud temperature measurements and to define the types of measurements that are inclined to be more reliable. The second goal is to provide a dataset that can be used to help to validate temperature and buoyancy features of cloud-resolving and mesoscale models. However, care must be taken when comparing the models with the aircraft observations of cloud temperature because of the inherent latency between the time a cloud initially forms and when it is usually sampled by an aircraft. For the most part, the data presented here are representative of clouds that do not contain unmixed cores, which are generally thought to occur in small convective clouds only very early in the cloud lifetime, or very close to cloud base (Blyth et al. 1988; Lawson and Blyth 1998). Exceptions to this generalization occur when instrumented gliders are able to make sustained observations in cloud updrafts. This is because the glider must identify the updraft early in its life cycle in order to maintain its ascent in cloud. A second exception occurs when very large diameter updrafts are sampled, such as the weak-echo regions of mesoscale cloud systems and supercells. When available, the in-cloud temperature measurements presented here are described in terms of the stage of the cloud life cycle.

2. Immersion and radiometric thermometry

Here we present a brief review of some of the salient factors considered in airborne immersion and radiometric thermometry. In particular, we discuss theoretical aspects, the response of immersion sensors in warm and supercooled clouds, and the application of measurements of temperature excess in calculations of cloud buoyancy. More complete theoretical treatments of immersion and radiometric thermometry can be found in the references cited in this paper.

a. Review of immersion thermometry

Independent and parallel paths followed in Russia and in the United States resulted in general agreement

in the physics and magnitude of errors associated with wetting of conventional immersion thermometers (Lenschow and Pennell 1974; Mazin and Shmeter 1977; Lawson and Cooper 1990).

Most airborne temperature probes use a sensing element immersed in the airstream. The temperature sensed by such an "immersion sensor" is influenced by several factors other than the static temperature of the air. The predominant corrections are those caused by compressional and viscous heating of the air and, in clouds or precipitation, by evaporative cooling if the sensor is wet. The effect of evaporative cooling on a wetted sensor depends on how much of the sensor is wet (Lenschow and Pennell 1974; Lawson and Cooper 1990). Also, even if the sensor does not get wet, air that comes in contact with a wetted housing will be cooled and may subsequently impact the sensor, causing measurement error (Lawson and Rodi 1992). The resulting sensor temperature will be between the wet-bulb temperature T_{wb} and dry-bulb recovery temperature T_r of the dynamically heated air (Pinus 1953; Telford and Warner 1962; Lenschow and Pennell 1974). Temperature T_r is the effective (i.e., average) temperature at the surface of the sensor when there is no net heat transfer to the airstream (Benedict 1984).

For a completely wetted sensor, Lawson and Cooper (1990) show that

$$T_{\mathrm{wb}} - T_r = \frac{-1}{AP_0}\left[e_s(T_{\mathrm{wb}}) - \frac{P_0}{P_\infty}e_\infty\right], \qquad (1)$$

where $e_s(T_{\mathrm{wb}})$ is the saturation vapor pressure at the sensor temperature, e_∞ and P_∞ are the water vapor pressure and total pressure, respectively, in the free airstream, P_0 is the total pressure at the surface of the sensor, and

$$A = \frac{C_p}{\varepsilon L_v}\left(\frac{\mathrm{Sc}}{\mathrm{Pr}}\right)^{0.56}\left[1 - \frac{\varepsilon e_s(T_{\mathrm{wb}})}{P_0}\right]$$

is the psychrometric parameter. In the definition of A above, C_p is the specific heat of air at constant pressure, ε is the ratio of molecular weight of water to the molecular weight of air, L_v is the latent heat of vaporization, Sc is the Schmidt number, and Pr is the Prandtl number. The quantity $T_{\mathrm{wb}} - T_r$ is the error caused by sensor wetting, and its absolute value is equal to the wet-bulb depression.

Using (1), Fig. 1 shows representative magnitudes of the errors in temperature measurement that would be caused by complete wetting of immersion sensors. Errors from sensor wetting can be about 1°–3°C at airspeeds of 100 m s^{-1}, for a sensor with a recovery factor near unity and for temperatures from −20° to +20°C.

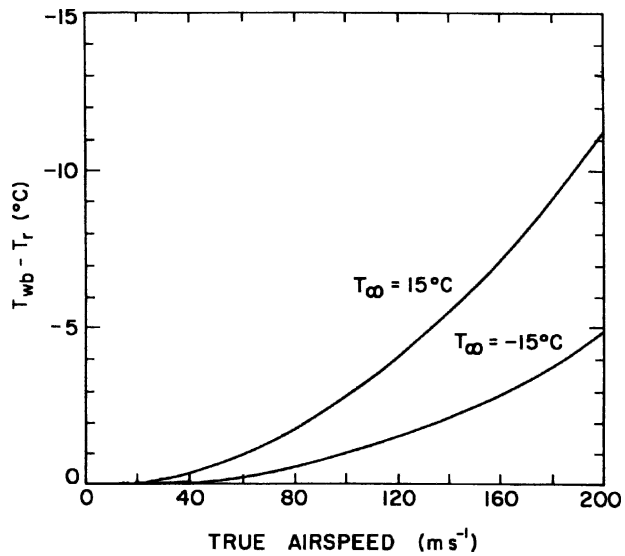

FIG. 1. Temperature error ($T_{\mathrm{wb}} - T_r$) for a wetted sensor as a function of true airspeed using (1) with $r = 1$ at two temperatures: −15° and +15°C.

The magnitude of the error is predicted to increase with airspeed, recovery factor, and temperature.

b. Review of radiometric thermometry

Understanding the problems resulting from sensor wetting led to the development of radiometric thermometers in the United States (Astheimer 1962; Albrecht et al. 1979; Nelson 1982; Lawson and Cooper 1990), Russia (Sinkevich 1979), and Great Britain (Nicholls et al. 1988). The radiometric thermometers discussed here measure the spectral radiance of an emitting gas (carbon dioxide or water vapor) and determine the corresponding emitter temperature. Details of radiometric thermometry can be found in, for example, Albrecht et al. (1979), Sinkevich (1979), and Nelson (1982). The principle of radiometric temperature measurement is based on the Planck relationship

$$P(\lambda, T) = \frac{2hc^2}{\lambda^5(e^{hc/\lambda kT} - 1)}, \qquad (2)$$

where $P(\lambda, T)$ is the spectral radiance measured at the detector, λ is wavelength, T is the temperature of the emitting gas, h is Planck's constant, c is the speed of light, and k is Boltzmann's constant. Solving for T in (2) gives the temperature of the gaseous emitters, assuming there are no other emitters that contribute significant radiance within the passband of the detector. Because it is impossible to eliminate all "contaminating" sources of radiation seen by the detector, the radiance from the emitting gas is generally "chopped" using an optical

chopper wheel, so that the detector alternately sees radiance from the emitting gas and a reference blackbody source emitting at a known temperature. Electronic synchronous detection is used to rectify the signal and to obtain the contribution from the emitting gas. Other assumptions that need to be considered are that all of the gaseous emitters are at the same temperature and that there are no other emitters in the sample volume, such as precipitation particles, that may emit spectral radiance at a temperature that is significantly different than that of the gas.

Radiometric thermometry has certain inherent advantages when compared with immersion thermometry. The temperature of the air is minimally disturbed by the sensor and there is little dynamic effect on the air temperature, except near the skin of the aircraft. The sensed temperature is a weighted average of the optical depth, which is a function of wavelength and concentration of the emitters. Because the radiometric temperature is a weighted average over the sample volume, aerodynamic effects associated with airflow near the aircraft are minimized because the sample volume is displaced from the surface. The length of the sample path also imposes a limit on the lower end of the scale of temperature fluctuations that can be measured, however, because the measurements are averages over the sample path. In contrast with immersion sensors, no thermal relaxation times are involved, and so relatively fast time responses are possible if the radiometric sample path is short. The measurements should be correct in water-saturated clouds that are devoid of large precipitation particles because the cloud-drop temperature is usually within about 0.1°C of the air temperature (Telford and Warner 1962).

On the other hand, when precipitation particles fall through an updraft or in subsaturated air, the temperature of the particles can be significantly different than the air temperature. For example, Hrgian (1961) has shown that for a raindrop with diameter of 2.7 mm and fall speed of 7.7 m s^{-1}, the temperature of the drop in a 25 m s^{-1} updraft is 0.5°C warmer than the air temperature. In converse, the temperature of a precipitation drop falling through subsaturated air, such as below cloud base into a hot, dry subcloud region, will be driven toward the wet-bulb temperature of the air and may be significantly cooler than its environment.

The selection of the wavelength at which a radiometric thermometer operates is governed by several factors. The wavelength should be well outside of the solar maximum to avoid unnecessary contamination from the sun. Even if the chosen wavelength is outside the solar maximum, care should be taken to shadow the radiometer from direct sun exposure. The gas should be a strong absorber/emitter at the chosen wavelength so that the sample path "goes black" within a relatively short distance from the aircraft. The chosen wavelength should be in a region in which a photodetector has a good signal-to-noise ratio.

Three different wavelengths were chosen for the radiometric thermometers from which measurements are reported in this paper. The radiometric thermometer described by Astheimer (1962) and Albrecht et al. (1979) operates in the carbon dioxide 14–16-μm band. The pathlength in clear air for the signal to go black in this waveband is on the order of 200–400 m, and in cloud it is about 50–100 m (Albrecht et al. 1979), because about one-half of the weighting will come from cloud-drop temperature (Nelson 1982).

The radiometric thermometer developed by Nelson (1982) and Nicholls et al. (1988) operates at 4.25 μm, where the spectral radiance at tropospheric temperatures is about 0.1 of that emitted in the 14–16-μm wave band. However, carbon dioxide is a very intense emitter in the vibration–rotation band at 4.25 μm, so that the path goes black within a relatively short distance (~10 m) from the aircraft; that is, virtually all of the observed radiance comes from a short distance from the sensor. In this case, the large majority of the radiometric temperature comes from the gas, except in the case in which the optical extinction coefficient exceeds about 100 km^{-1} (Lawson 1988). The significantly reduced radiance at 4.25 μm when compared with the 14–16-μm band is offset by the more sensitive detector used at 4.25 μm (Nelson 1982).

The radiometer developed by Sinkevich (1979) operates in the water vapor absorption band centered at 6.3 μm. Sinkevich (1981) has shown that

$$\frac{\partial P(\lambda_{15}, T)}{\partial T} \approx \frac{\partial P(\lambda_{6.3}, T)}{\partial T},$$

where λ_{15} = 15 μm and $\lambda_{6.3}$ = 6.3 μm. Thus, the changes in emitted energy due to changes in temperature in these two wavebands are approximately equal. Like the radiometer operated at 15 μm, the pathlength in clear air of the 6.3-μm radiometric thermometer varies from several hundreds of meters to kilometers. In convective clouds, the range is from about 50 to 100 m, depending on the magnitude of the optical extinction coefficient.

Radiometric thermometry also has some disadvantages. Radiometric thermometers are large and fairly costly to build, calibrate, and maintain. The solid-state photodetectors require either thermoelectric or cryogenic cooling. The clear-air baseline of radiometric thermometers tend to drift in airborne applications,

probably because of thermal gradients within the housing that cause stray radiance to be seen by the detector. In addition, as can be seen from (2), $\partial P(\lambda, T)/\partial T$ results in a nonlinear output that decreases with decreasing temperature. This results in a decrease in sensitivity that, for solid-state photodetectors, becomes significant when atmospheric temperatures are less than approximately $-30°$ to $-40°$C, depending on the type of photodetector and the magnitude of (cryogenic or thermoelectric) cooling of the detector. This can limit the usefulness of radiometric thermometry in the upper troposphere and stratosphere, and in the polar regions in the wintertime.

c. *Sensor response in warm and supercooled clouds*

Lawson and Rodi (1987) demonstrate that the location of the temperature sensor in the National Center for Atmospheric Research (NCAR) reverse-flow probe (Rodi and Spyers-Duran 1972) gets wet in warm clouds but does not get wet in supercooled clouds. They did this by replacing the platinum temperature sensor with a conductivity element that was highly sensitive to the presence of liquid water. They concluded from icing tunnel tests that the conductivity element did not get wet in supercooled clouds because water froze on the housing instead of streaming back to the (reverse flow) entrance, as was the case in warm clouds.

The icing tunnel tests reported by Lawson and Rodi (1987) have been supported by aircraft observations collected in both in Russia and the United States in warm and supercooled clouds. Table 1 summarizes the means and standard deviations in the differentials between radiometric and immersion temperature measurements in warm and cold cumulus congestus clouds observed in Russia. The data in the table show that immersion temperature measurements are systematically colder than radiometric values in warm clouds by about 2.5°C, whereas the two probes measure nearly the same mean value in supercooled clouds. Figure 2 shows an example of measurements taken in warm and supercooled cumulus clouds in Russia by a reverse-flow-type thermometer with a small thermistor sensor

TABLE 1. Measurements of radiometric temperature minus immersion temperature in warm and cold cumulus congestus clouds investigated by a Russian IL-14 research aircraft.

	Warm cloud	Cold (supercooled) cloud
Mean temperature difference	2.3°C	0.2°C
Std dev	0.7°C	0.3°C
No. of clouds	18	19

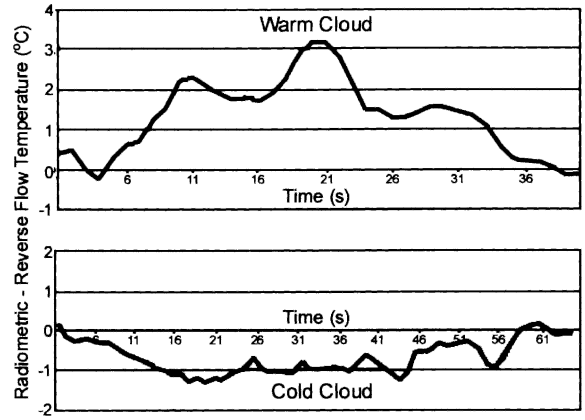

FIG. 2. Time series of 6.3-μm radiometer minus reverse-flow temperature measurements in the (top) warm portion and (bottom) supercooled portion of a small cumulus cloud, with a liquid water content of about 0.5 g m^{-3} in warm cloud and 1 g m^{-3} in cold cloud. Cloud edges are at the extremities of each time series. The data were collected in northwestern Russia by an IL-14 research aircraft.

and a 6.3-μm radiometer (Zvonarev and Sinkevich 1991). The top panel in Fig. 2 shows measurements in a warm cumulus cloud at $T = 16°$C and liquid water content of about 0.5 g m^{-3}. The bottom panel in Fig. 2 shows measurements in a supercooled cumulus cloud at $T = -12°$C and a liquid water content of about 1.0 g m^{-3}. In this case the radiometric temperature is about 1°C colder than the immersion temperature. We cannot predict whether the immersion thermometer temperature should be warmer or colder in this situation. Accretion of ice on the housing of the thermometer tends to warm the air because of the latent heat of fusion, but also evaporation of air passing over ice will tend to cool the air through sublimation.

The data shown in Fig. 2 are examples of maximum differentials in measurements observed between radiometric and the Russian immersion thermometers (described above) in warm ($\sim$3°C) and cold ($\sim -1°$C) clouds. As shown in Table 1, the mean value of temperature measurements from the radiometer is about 2.5°C warmer than the immersion thermometer, which, as shown in Fig. 1, is the maximum predicted cooling due to sensor wetting at an airspeed of 100 m s^{-1} and a temperature of 15°C. In this case, however, the Russian twin-engine IL-14 turboprop research aircraft was operated at 70 m s^{-1} and the cloud temperature was 21°C, which corresponds in Fig. 2 to a maximum cooling of 2°C from sensor wetting. The fact that the temperature differential between the immersion sensor and the radiometer exceeds the theoretical maximum is not cause for concern, because the difference of 0.5°C is well within the uncertainty limits of the radiometric mea-

surements and assumptions in the development of the theoretical curves shown in Fig. 1.

Figure 3 shows examples of scatterplots of measurements from the NCAR reverse-flow thermometer and the Ophir 4.25-μm thermometer (Nelson 1982) in warm and supercooled regions of a stratus cloud containing only about 0.1–0.2 g m^{-3}. In this case, the aircraft climbed from the warm portion of cloud, through the freezing level, and into the supercooled portion of cloud. The radiometric minus immersion sensor temperature difference between the measurements in the warm and supercooled portions of this cloud ranges from 0.5° to 1°C. Although the magnitude of temperature measurement difference is different in the two cases (i.e., Figs. 2 and 3), it is within the theoretical range expected for sensor wetting shown in Fig. 1. The difference between the magnitudes in Figs. 2 and 3 may be due to the percentage of the sensor that is getting wet, because the magnitude of the error in temperature measurement is proportional to the percentage of the sensor that is wet. The Russian reverse-flow thermometer used a small thermistor, whereas the NCAR design used a 1-m coiled platinum wire. It is possible that not all of the wire was wet, and it is somewhat more likely that wetting of the thermistor would result in complete wetting of the sensor.

Figure 4 shows a plot of temperature difference between the Ophir radiometric thermometer and the NCAR reverse-flow probe as a function of liquid water content in a warm cumulus cloud observed in Louisiana. The data in Fig. 4 show that the temperature difference increases with increasing liquid water content. One possible explanation for this is that more of the 1-m platinum wire gets wet as the liquid water content increases. If this is the case, it may not always be possible to predict the magnitude of error due to sensor wetting unless the sensor is always completely wet.

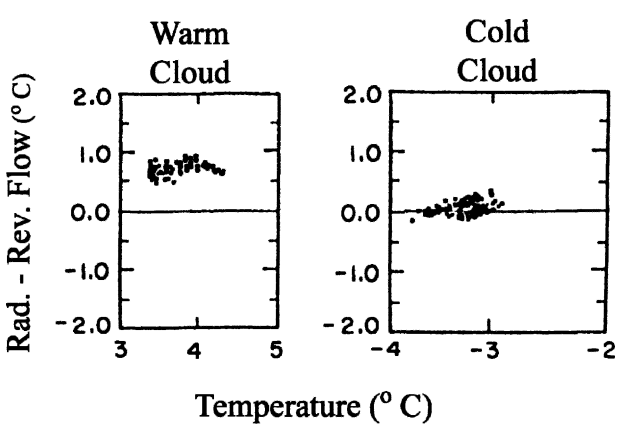

FIG. 3. Plots showing 4.25-μm radiometer minus reverse-flow temperature measurements in (left) warm and (right) supercooled stratus cloud with liquid water content of 0.1–0.2 g m^{-3} observed in Louisiana by the NCAR King Air.

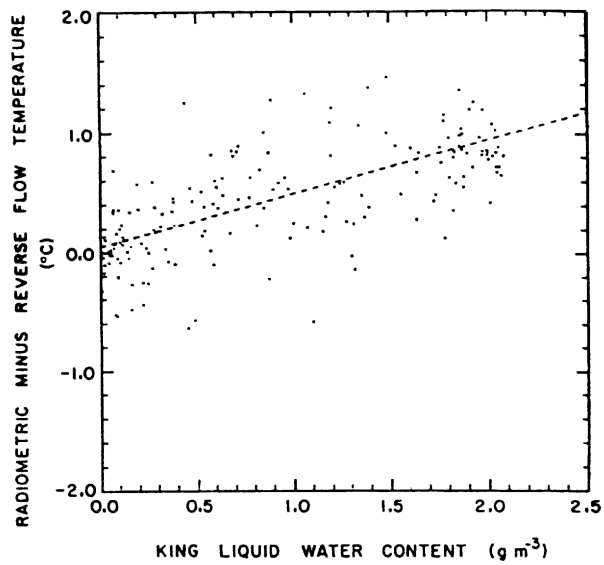

FIG. 4. The difference between measurements from the Ophir 4.25-μm radiometer and reverse-flow immersion thermometers, plotted as a function of liquid water content measured by a Commonwealth Scientific and Industrial Research Organization King probe (King et al. 1978), manufactured by Particle Measuring Systems, Inc. Data were collected by the NCAR King Air in a cumulus cloud investigated in Louisiana on 7 Nov 1985.

d. Application to cloud buoyancy

In this paper we present measurements of temperature excess in clouds; measurements of cloud buoyancy are more useful for understanding the physics of cloud development and decay and for comparison with cloud models, however. Cloud buoyancy B is defined as $B = \Delta T_v - B_l$, where $\Delta T_v = T_v - T_{ve}$ and the component of buoyancy due to water loading is $B_l = T_{ve} r_l$ (Wei et al. 1998). Here, T_v and T_{ve} are, respectively, the virtual temperature in cloud and in the environment, and r_l is the total liquid water mixing ratio. Measurements of r_l in growing cumulus clouds suggest that r_l is typically on the order of 1 g kg^{-1} (Cooper and Lawson 1984; Blyth et al. 1988), equating to a value of B_l of about 0.3 K. Values of r_l of about 2 g kg^{-1} are observed in adiabatic cores of growing cumulus congestus (Lawson and Cooper 1990; Lawson and Blyth 1998), with much higher adiabatic values, on the order of 10 g kg^{-1}, only observed in the weak-echo region of supercells (Musil et al. 1986). Wei et al. (1998) found that the maximum value of B_l was about 0.5 K in warm regions of tropical convective clouds that were not precipitating heavily. These measurements suggest that, except in supercells and cells containing heavy precipitation, liquid water

loading contributes less than 0.5 K to total buoyancy in convective cells. We chose to neglect the effects of liquid water loading in the data presented in this paper because measurements of cloud liquid water and precipitation contain significant uncertainties themselves (see Wei et al. 1998).

3. Measurements in convective clouds

The measurements presented in this paper are from airborne penetrations of cumulus clouds. Uncertainty analyses conducted by Sinkevich (1979), Cooper (1987), Lawson (1988), and Blyth et al. (1988) provide a basis for estimating uncertainty in these measurements. From this information, we estimate that about 95% of the measurements presented here should be accurate to within about ±0.5°C. This uncertainty estimate includes the contributions of calibration, installation, and data recording. Most of the measurements come from radiometric thermometers that have been carefully calibrated (Sinkevich 1984; Sinkevich 2001; Lawson 1988).

Additional measurements are from a wet-bulb thermometer in warm clouds in the Caribbean and a reverse-flow thermometer (Rodi and Spyers-Duran 1972) determined to be reliable in supercooled clouds with liquid water contents of less than approximately 3 g m^{-3} (Lawson and Rodi 1987; Blyth et al. 1988; Lawson and Cooper 1990). The wet-bulb thermometer is considered to be reliable, because it is measuring wet-bulb temperature, which is thought to be within about 0.1°C of the cloudy air temperature in warm clouds with weak to moderate updrafts (Telford and Warner 1962). Reverse-flow temperature measurements on the glider operated by NCAR are also presented and are reliable in all clouds. This is because the true airspeed of the NCAR glider is <40 m s^{-1}, so that the error predicted from sensor wetting using (1) is <0.3°C.

Table 2 is a summary compilation of temperature measurements presented in this paper. The data in Table 2 have been sorted according to cloud type and (if information is available) by the age of the convective cell, that is, growing, mature, and dissipating stages. The geographic location of the measurements is included, and, wherever possible, an indication of the vigor of the cloud system is given, as is the number of cloud penetrations.

The data in Table 2 were collected and processed using differing methods, and distinctions need to be made in order to compare the results. In-cloud temperature excess has an inherent error associated with the measurement of environmental temperature. The error in temperature measurements in clear air has been reported to be 0.3°C (Lawson 1988); however, environmental temperature in the vicinity of clouds can have significant structure and also can be affected by vertical motions, mixing, and detrainment of cloudy air from the clouds themselves. Different techniques were used in Table 2 to determine environmental temperature. Most of the environmental temperatures in Table 2 were determined by averaging clear-air temperatures measured on both sides of the clouds, such as the 20-s averaging technique described by Wei et al. (1998) and Igau et al. (1999). Studies listed in Table 2 that used this technique, or a close variation of this technique (i.e., differences may be a slightly different averaging period or manual editing to exclude regions near cloud that appeared to be affected by cloudy air) include Cooper et al. (1982), Jorgenson and LeMone (1989), High Plains Experiment 1978 (HIPLEX) feeder cells, Louisiana 1985 cumulus congestus, and the Russian studies. Average environmental temperatures for studies presented by Malkus (1954) and Musil et al. (1986) were determined by us by averaging the plots of environmental temperature over ~60 s, based on the figures shown in their papers. Environmental temperature data for the NCAR glider ascents (Heymsfield et al. 1978; Paluch and Breed 1984) were determined from radiosonde soundings launched in close proximity to the clouds.

The type of research aircraft, flight profiles, and scientific objectives themselves influence the measurements. For example, the measurements shown in Table 2 that were collected using an instrumented glider are biased toward convective clouds that were investigated very early in their lifetime, often when they still had unmixed cores. This bias is because the NCAR glider has a sink rate of about 1 m s^{-1} and can make a successful ascent only when there is a sustained updraft, which, in the case of cumulus congestus, is very early in the cloud lifetime when it is positively buoyant. On the other hand, the measurements made during the Tropical Ocean and Global Atmosphere Coupled Ocean–Atmosphere Response Experiment (TOGA COARE) (Igau et al. 1999; Wei et al. 1998) were collected by the National Science Foundation Electra turboprop aircraft operated by NCAR and the crew were not attempting to select growing clouds. In this case, the aircraft was flying relatively straight legs through large cloud systems in the Tropics. The TOGA COARE data shown in Table 2 were analyzed especially for this study; the results are in general agreement with the findings reported in Igau et al. (1999) and Wei et al. (1998). The procedure used here to process the TOGA COARE data consisted of objectively sorting updraft and downdraft regions, which were identified by an average posi-

TABLE 2. Summary results of in-cloud temperature measurements from various research projects in Russia and the West. Here, CuCg is cumulus congestus, Pos is positive, Neg is negative, Cld is cloud, WER is weak-echo region, RFT is reverse-flow thermometer, Rad is radiometer, NHRE is National Hail Research Experiment, CCOPE is Cooperative Convective Precipitation Experiment, and TAMEX is Taiwan Area Mesoscale Experiment. "Stabilized" is a term used by the Russian scientist on the research aircraft that refers to a dwell period that some clouds experience between growing and dissipating stages (Byers and Braham 1949).

No.	Reference	Location	Cloud type	Sensor type	Obs level (°C)	Cloud stage	Max ΔT (°C)	Pos avg ΔT (°C)	Cld avg ΔT (°C)	Neg max ΔT (°C)	Neg avg ΔT (°C)	Comments
1	Malkus (1954)	Caribbean	CuCg	Wet bulb	+17	Lifetime	2.5	2	−0.1			Two clouds lifetime
2	Heymsfield et al. (1978)	Eastern CO (NHRE)	Feeder cells	RFT	0 to −30 (4.5–8.5 km AGL)	Developing	4	2.5				Glider ascents
3	Cooper et al. (1982)	Southeastern MT (HIPLEX 1977–80)	CuCg	NCAR RFT	−5 to −15		2.8		0.2			Project avgs
4	Paluch and Breed (1984)	Southeastern WY (NHRE)	Feeder cell	RFT	−2 to −30 (4.5–8.5 km)	Developing	3.2	2.5				Glider ascent
5	Musil et al. (1986)	Southeastern MT (CCOPE 1981)	WER in supercell	RFT	−8 to −15	Mature	6–8	6				One penetration with T-28 armored aircraft
6	Jorgensen and LeMone (1989)	Western Pacific (TAMEX)	Mesosystem	15-μm Rad.	+25–0		3.5		0.2			Random clouds
7	This work	Western KS (HIPLEX 1978)	Feeder cells	NCAR RFT	−15	Developing	3.8	1.8	1.2			Cloud avgs unmixed core
8	This work	LA (1985)	CuCg	4.25-μm Rad.	+12	Developing	3.1	2.1	1.4			Cloud avg unmixed core
9	This work	Northwestern USSR (1977–87)	CuCg	6.3-μm Rad.	Cloud base to 1 km above	Developing	2.7	1.0	0.2	−1.3	−0.5	46 penetrations
						Stabilized	2.1	0.7	0.1	−1.7	−0.5	98 penetrations
						Dissipating		0.7	−0.1	−1.7	−0.7	43 penetrations
					1–2 km above cloud base	Developing	2.5	1.2	0.5	−1.1	−0.1	86 penetrations
						Stabilized	3.0	1.0	0.3	−2.7	−0.4	88 penetrations
						Dissipating	1.6	0.5	−0.1	−1.9	−0.7	33 penetrations
					2–3 km above cloud base	Developing	4.1	1.5	0.7	−0.9	−0.1	48 penetrations
						Stabilized	4.0	1.4	0.4	−3.7	−0.5	48 penetrations
						Dissipating	1.9	0.8	0.2	−1.5	−0.4	60 penetrations
					3–4 km above cloud base	Developing	2.8	1.4	0.7	−0.3	0.0	10 penetrations
							Up max	Up avg	Down min	Down avg		
10	Igau et al. (1999), Wei et al. (1998), and this work	Equatorial Pacific (TOGA COARE 1992–93)	Meso-CuCg	4.25-μm Rad.	0.1–1.9 km above cloud base		2.9	0.8	−0.9	0.6		41 penetrations
					1.9–3.7 km above cloud base		3.4	0.4	−1.6	0.4		194 penetrations
					3.7–5.2 km above cloud base		2.8	0.8	−0.4	0.3		28 penetrations

tive or negative vertical velocity of at least 1 m s^{-1} over a minimum of 500 m. Therefore, clouds were investigated in nearly all stages of development and were not classified as to their stage of development.

Even when an aircraft is attempting to investigate clouds at a certain stage in their development, the results will be somewhat biased by the type of aircraft and the flight profile. The data in Table 2 from Russia were mostly collected in isolated cumulus congestus clouds using the IL-14 research aircraft. In this case, it takes several minutes to identify a cloud and to maneuver to penetrate the cloud. The lifetimes of isolated, continental cumulus congestus are generally on the order of 20–30 min (Cooper and Lawson 1984; Schemenauer and Isaac 1984). When a candidate cloud is visually identified, it is already in its developing stage, and so measurements will usually be biased toward the latter part of the developing stage. In converse, when a highly maneuverable jet aircraft is used to investigate feeder cells associated with a multicell thunderstorm, such as the Learjet model 24 operated by Colorado International Corporation and used in the HIPLEX, the aircraft is in position to maneuver rapidly to cells that often propagate in a systematic manner. In this case, the rapidly growing cells may be penetrated early in their developing stage and may often contain unmixed cores (Lawson et al. 1980). Of interest is that the NCAR glider, which has an airspeed of about 30 m s^{-1}, was also flown in such a manner that it often encountered unmixed cores in feeder cells (Heymsfield et al. 1978). This fact is because an experienced glider pilot can often identify and penetrate feeder cells early in their development, and the glider would soon lose lift if it did not remain in the unmixed core of the updraft. In our interpretation of the data presented in Table 2, we take into account how the types of aircraft and methods likely influenced the dataset.

The following general conclusions are drawn from the data shown in Table 2:

1) For studies 1, 3, 6, and 9, in which data were collected over all stages of the lifetimes of cumulus clouds, the cloud-average temperature excess is about 0.2°–0.3°C. (To compute the average temperature excess over cloud lifetime for the measurements from Russia, the cloud averages for developing, stabilized, and dissipating stages at all altitudes were averaged.) Also, based on the Russian measurements, where the clouds were systematically classified according to the three stages of their lifetime, the small positive temperature excess averaged over cloud lifetime is attributable to significantly stronger values in developing stages when compared with weak negative values in dissipating stages. This result can also be inferred from the TOGA COARE data where the maximum positive temperature excesses in updrafts were about 2–7 times the maximum negative values in downdrafts. Wei et al. (1998) found that the average virtual temperature excess in both updrafts and downdrafts in TOGA COARE was positive—on the order of 0.5°C in updrafts and 0.2°C in downdrafts—and that the contribution of precipitation loading was <0.5°C.
2) The maximum temperature excess in cumulus congestus clouds, including feeder cells (studies 1, 2, 3, 4, 7, 8, 9, 10), is 2.5°–4°C.
3) Based on studies 1, 2, 3, 4, 7, 8, 9, and 10 in cumulus congestus clouds and feeder cells with unmixed cores (i.e., investigated very early in their lifetime), the average temperature excess in the updraft region is 2°–3°C, as compared with 0.5°–1.5°C in clouds that are selected randomly, or where the selection process prevents them from being reached early in the cloud lifetime.
4) Based on reverse-flow measurements from an armored T-28 research aircraft operated by the South Dakota School of Mines and Technology (Musil et al. 1986), the maximum temperature excess in the main supercooled updraft (i.e., weak-echo region) of a supercell is on the order of 6°–8°C. The reverse-flow temperature measurements reported by Musil et al. (1986) were collected in the weak-echo region of a supercell storm, where the updraft velocity peaked at 50 m s^{-1} and the liquid water content reached 6 g m^{-3}. Measurements in this region with very high liquid water may have been influenced by sensor wetting, because the wetting mechanism of the reverse-flow probe involves water streaming along the outside of the housing (Lawson and Rodi 1987). The maximum temperature (cooling) error predicted by (1) for the armored T-28 is about 2°C, and so the maximum temperature excess in this case may have been as large as 10°C. This value is not unreasonable, because the updraft had microphysical characteristics usually associated with an unmixed core, and the adiabatic temperature excess in the updraft using actual cloud base measurements is predicted to be about 10°C.
5) Based on measurements collected in cumulus congestus from Russia, which give the most comprehensive picture of data as a function of altitude, positive temperature excess increases from cloud base up to about 3 km above cloud base in the developing and stabilized stages. Positive temperature excess in dissipating clouds and negative temperature excess in

all stages, on the other hand, do not display any systematic trends as a function of altitude.

6) Although updraft velocities are typically greater over land than over oceans and maximum updraft velocities in the lower troposphere over land are more than double those over oceans (Jorgensen and LeMone 1989; Musil et al. 1986), temperature excess in updrafts over land is only slightly larger than over oceans. Except for the values observed in the main updrafts of supercells, the maximum temperature excess over land is on the order of 4°C, whereas over oceans it is 2.5°–3.5°C. The average maximum temperature excess (or maximum positive average for the Russian data) over land is 0.7°–2.5°C, whereas the TOGA COARE updraft average temperature increase sampled in the lower troposphere over the ocean in randomly selected clouds is 0.4°–0.8°C.
7) Measurements of average temperature excess in cumulus congestus clouds using radiometric thermometers developed in the United States and the (former) Union of Soviet Socialist Republics (USSR) are very similar in magnitude.

4. In-cloud temperature structure

In addition to the general body of temperature measurements shown in Table 2, there have been some measurements of temperature structure in cumulus clouds that may shed some light on the entrainment and mixing process. Baker et al. (1984) discuss a concept of entrainment and mixing in cumulus clouds that is based in part on the Broadwell and Briedenthal (1982) mixing model. In this context, "blobs" of dry air on the order of a few hundred meters are entrained into cloud and form ribbons that take a few minutes to thoroughly mix down to the millimeter scale. This process can result in relatively large inhomogeneities in cloudy air temperature on scales from hundreds of meters to a few centimeters.

Sinkevich (2001) shows simultaneous measurements with three 6.3-μm temperature radiometers—two pointed horizontally outward from the aircraft and one pointed downward. An example of three radiometric temperature measurements during a pass through a small cumulus congestus is shown in Fig. 5. It can be seen from the data in Fig. 5 that the shapes and magnitudes of the temperature fluctuations recorded by all three radiometers are similar. This gives support to the validity of the calibration of the radiometers. Also, because in this case the pathlength of the radiometers is on the order of 50 m, the measurements give some estimate of the size and shape of eddies that are 100 m and larger, which appear to be on the order of 300–400 m in this example. Using this unique three-radiometer technique, measurements are made that describe the shape and distribution of the larger (>100 m) eddies in cumulus clouds. The measurements provide some information on the three-dimensional structure of temperature in cumulus clouds.

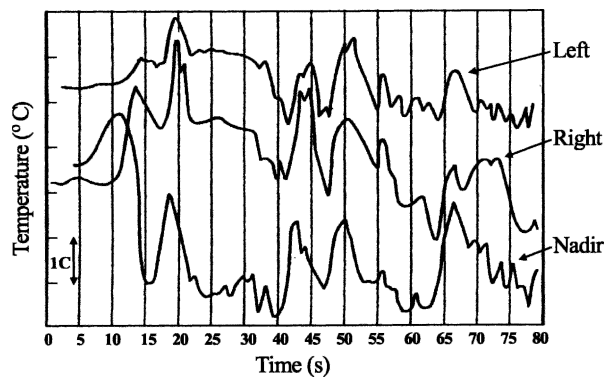

FIG. 5. Time series showing simultaneous temperature measurements for one vertically pointing and two horizontally pointing 6.3-μm radiometers installed on the Russian IL-14 research aircraft. Measurements were made in a cumulus congestus cloud in northwest Russia.

Figure 6 is a histogram of the locations at which the maximum temperature excess occurred in each of 20 cumulus congestus clouds investigated in northwest Russia. The clouds were either developing or mature and ranged from 2 to 3 km in height. The aircraft penetrations were conducted in the upper 1 km of the clouds. The clouds were each divided into six equal

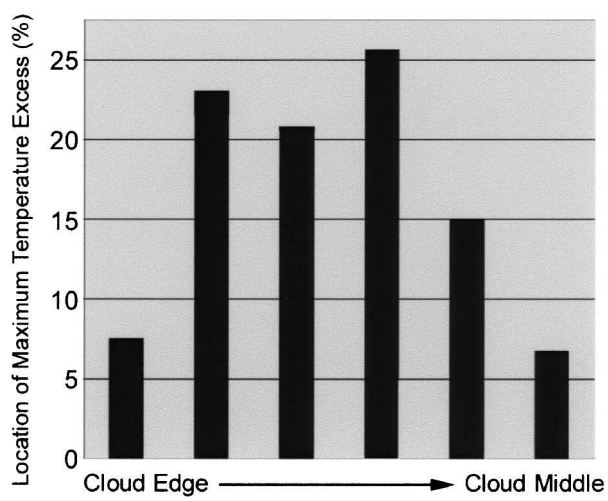

FIG. 6. Histogram of locations of temperature excess in cumulus clouds as a function of position within the clouds. Data are shown for penetrations of 20 developing and mature cumulus congestus clouds in northwest Russia. Clouds were penetrated within the upper 1 km of clouds that were 2–3 km in height.

sections between cloud edge and cloud middle. The data show that the maximum temperature excess is not observed in the center of cloud but instead is found between cloud center and cloud edge. While these results may at first seem counterintuitive, they are not without precedent. For example, as shown in Fig. 7, Blyth et al. (1988) suggest a model of entrainment and mixing in small cumulus in which thermals may erode into a doublet near cloud top. This process could explain the observations suggesting that the maximum temperature excess is most often observed between cloud edge and cloud middle. Another possibility is that the offset is a result of sampling clouds that were primarily building on the upwind and decaying on the downwind side of cloud. The location of highest liquid water content would likely be nearer to the upshear side of the cloud. In either case, the results may be consistent with the concept of entrained air being brought back into the updraft.

Baker (1992) showed that the spacing of cloud drops in cumulus clouds is inhomogeneous down to the centimeter scale, which is consistent with the Baker et al. (1984) mixing model. Haman et al. (1997, 2001) show in-cloud temperature measurements using a fine-wire thermocouple with a time response on the order of 10^{-4} s. The sensor is protected mechanically, and the measurements indicate that it is protected from wetting in most clouds. The measurements presented by Haman et al. are intended to show small-scale temperature fluctuations in clouds, not average excess cloud temperature measurements. The small-scale temperature measurements show relatively large fluctuations in temperature over length scales on the order of 1°–2°C on scales of 2–3 cm. Sharp temperature fluctuations over short length scales are also predicted by the cumulus-mixing model put forth by Baker et al. (1984). More comprehensive measurements of temperature, cloud-drop spacing, and water vapor are required, however, before the mixing process in cumulus clouds can be adequately explained.

5. Summary and discussion

In-cloud temperature measurements are vital for understanding cloud physical processes. However, immersion thermometry has been plagued by errors, predominately due to sensor wetting, since research aircraft first started making cloud measurements in the first half of the twentieth century. To date, it has not been convincingly demonstrated that an immersion thermometer can be designed that is totally immune to errors associated with sensor wetting. Attempts to minimize errors associated with in-cloud immersion thermometry continue, and there appears to be progress in this direction (e.g., Haman et al. 1997, 2001).

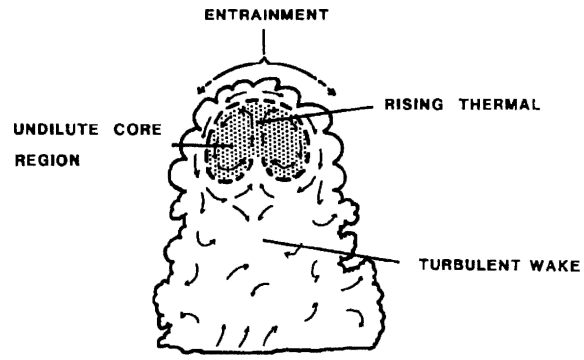

FIG. 7. Conceptual drawing of a developing cumulus cloud showing a rising thermal and possible circulations near cloud top (from Blyth et al. 1988).

Radiometric thermometry was introduced in the early 1960s and has the intrinsic advantage that there is not an immersion sensor that can get wet. Reliable radiometric temperature measurements are not easy to make, however, because the instruments built to date require very careful calibration and understanding of potential sources of error. Two major challenges that present themselves to radiometric thermometry are 1) the signal-to-noise ratio is typically very small and 2) the response of the detector is nonlinear and appears to vary over time, so that frequent calibration of the gain term is required. As a result, there are only a few in-cloud radiometric temperature measurements of cumuli presented in the literature that we have found to be reliable (e.g., Sinkevich 2001; Lawson and Cooper 1990; Wei et al. 1998). These measurements required very careful examination of the data, including careful comparisons with well-calibrated immersion thermometers outside of clouds, and comparisons with adiabatic cloud values to ascertain validity of the radiometric measurements. It may be possible to construct a reliable, robust temperature radiometer that does not require expert attention, but, to date, it has not been accomplished. It is, however, an undertaking that has the potential to provide significant advances in cloud physics.

The in-cloud temperature measurements presented in this paper were drawn from sources that we found to be reliable but not without error. Our best estimate is that, when the radiometric temperature is set equal to a well-calibrated immersion thermometer outside of cloud, the mean radiometric temperature error is on the order of 0.5°C. Because the gain term does not change over the time period of a cloud pass, the relative error in temperature fluctuations within a cloud pass may be as small as 0.1°C. Because there is no in-cloud

temperature standard with which to compare, the uncertainty in the estimate of mean radiometric temperature error could easily be as large as the estimate of the error itself. In some cases, for example, the armored T-28 reverse-flow measurements in the main (supercooled) updraft region of a supercell, the error in temperature could be as large as a few degrees Celsius. The in-cloud temperature excess is so large in this case, however, that it is still valuable to report the measurements.

It is worth noting that the radiometric measurements of temperature excess in small cumulus made independently in Russia and the West are in good general agreement. This fact suggests that these measurements have credence, but it does not eliminate the possibility that instrumentation errors led to similarly misleading results in both cases. Also, it must be kept in mind that all of the in-cloud temperature measurements are biased by the aircraft sampling strategy, which is usually to select candidate clouds based on visual appearance. This approach results in an inherent latency in the time the cloud is selected and the time it is sampled. Thus, temperature excess averaged over a cloud lifetime may be biased in some unknown manner.

Based on measurements presented in Table 2, we summarize our results as follows: The cloud temperature excess averaged over cloud lifetime is 0.2°–0.3°C, but this small positive value may not be significant because of some unknown instrument or experimental bias error. Cumulus congestus clouds selected at random (or unknown) times in their life cycle have a temperature excess of 0.5°–1.5°C; cumulus congestus clouds selected early in their life cycle, which may (or may not) contain unmixed cores, have a temperature excess of 2°–3°C. Cumulus congestus have a maximum temperature excess of 2.5°–4°C. The temperature excess in cumulus congestus over land is about 1°C larger than that for cumulus congestus observed over the ocean. Large convective cells associated with supercells have maximum temperature excess on the order of 6°–10°C.

Acknowledgments. This work was performed under funding from the National Science Foundation Grants ATM-9904710 and ATM-0244731. Any opinions, findings, and conclusions or recommendations expressed in this material are those of the authors and do not necessarily reflect those of the National Science Foundation.

REFERENCES

Albrecht, B. A., S. K. Cox, and W. H. Schubert, 1979: Radiometric measurements of in-cloud temperature fluctuations. *J. Appl. Meteor.,* **18,** 1066–1071.

Astheimer, R. W., 1962: An infrared radiation air thermometer. *Proc. University of Michigan Symp. on Remote Sensing of Environment*, Ann Arbor, MI, Willow Run Laboratories, University of Michigan.

Baker, B. A., 1992: Turbulent entrainment and mixing in clouds: A new observational approach. *J. Atmos. Sci.,* **49,** 387–404.

——, R. E. Breidenthal, T. W. Choularton, and J. Latham, 1984: The effects of turbulent mixing in clouds. *J. Atmos. Sci.,* **41,** 299–304.

Barrett, E. W., and H. Riehl, 1948: Experimental verification of entrainment of air into cumulus. *J. Meteor.,* **5,** 304–307.

Benedict, R. P., 1984: *Fundamentals of Temperature, Pressure, and Flow Measurements*. John Wiley and Sons, 532 pp.

Blyth, A. M., 1993: Entrainment in cumulus clouds. *J. Appl. Meteor.,* **32,** 626–641.

——, W. A. Cooper, and J. B. Jensen, 1988: A study of the source of entrained air in Montana cumuli. *J. Atmos. Sci.,* **45,** 3944–3964.

Broadwell, J. E., and R. E. Breidenthal, 1982: A simple model of mixing and chemical reaction in a turbulent shear layer. *J. Fluid Mech.,* **125,** 397–410.

Byers, H. R., and R. R. Braham, 1949: *The Thunderstorm*. U.S. Government Printing Office, 287 pp.

Cooper, W. A., 1987: The Ophir radiometric thermometer: Preliminary evaluation. NCAR Tech. Note NCAR/TN-292+STR, 54 pp.

——, and R. P. Lawson, 1984: Physical interpretation of results from the HIPLEX-1 Experiment. *J. Climate Appl. Meteor.,* **23,** 523–540.

——, ——, A. R. Rodi, and T. A. Cerni, 1982: Cloud physics investigations. Tech. Rep. AS 142, University of Wyoming, 129 pp.

Haman, K. E., A. Makulski, S. P. Malinowski, and R. Busen, 1997: A new ultrafast thermometer for airborne measurements in clouds. *J. Atmos. Oceanic Technol.,* **14,** 217–227.

——, S. P. Malinowski, B. D. Struś, R. Busen, and A. Stefko, 2001: Two new types of ultrafast aircraft thermometer. *J. Atmos. Oceanic Technol.,* **18,** 117–134.

Heymsfield, A. J., P. N. Johnson, and J. E. Dye, 1978: Observations of moist adiabatic ascent in northeast Colorado cumulus congestus clouds. *J. Atmos. Sci.,* **35,** 1689–1703.

Hrgian, A. H., 1961: *Cloud Physics*. Hydrometeoizdat, 459 pp.

Igau, R. C., M. A. LeMone, and D. Wei, 1999: Updraft and downdraft cores in TOGA COARE: Why so many buoyant downdraft cores? *J. Atmos. Sci.,* **56,** 2232–2245.

Jorgensen, D. P., and M. A. LeMone, 1989: Vertically velocity characteristics of oceanic convection. *J. Atmos. Sci.,* **46,** 621–640.

King, W. D., D. A. Parkin, and R. J. Handsworth, 1978: A hot-wire liquid water device having fully calculable response characteristics. *J. Appl. Meteor.,* **17,** 1809–1813.

Klaassen, G. P., and T. L. Clark, 1985: Dynamics of the cloud-environment interface and entrainment in small cumuli: Two-dimensional simulations in the absence of ambient shear. *J. Atmos. Sci.,* **42,** 2621–2642.

Krueger, S. K., C. W. Su, and P. A. McMurtry, 1997: Modeling entrainment and fine-scale mixing in cumulus clouds. *J. Atmos. Sci.,* **54,** 2697–2712.

Lawson, R. P., 1988: The measurement of temperature from an aircraft in cloud. Ph.D. dissertation, University of Wyoming, 336 pp. [Available from University of Wyoming, P.O. Box 3038, Laramie, WY 82071.]

——, and A. R. Rodi, 1987: Airborne tests of sensor wetting in a

reverse-flow temperature probe. Preprints, *Sixth Symp. on Meteorological Observations and Instrumentation*, New Orleans, LA, Amer. Meteor. Soc., 253–256.

——, and W. A. Cooper, 1990: Performance of some airborne thermometers in clouds. *J. Atmos. Oceanic Technol.,* **7,** 480–494.

——, and A. R. Rodi, 1992: A new airborne thermometer for atmospheric and cloud physics research. Part I: Design and preliminary flight tests. *J. Atmos. Oceanic Technol.,* **9,** 556–574.

——, and A. M. Blyth, 1998: A comparison of optical measurements of liquid water content and drop size distribution in adiabatic regions of Florida cumuli. *Atmos. Res.,* **47–48,** 671–690.

——, L. G. Davis, and D. S. Treddenick, 1980: Airborne cloud physics and seeding: Investigations by Colorado International Corporation in HIPLEX. 1977–1980. U.S. Water and Power Resources Service Final Rep. Contract 83-V0004, Division of Water Resources Management, 240 pp.

LeMone, M. A., 1983: Momentum transport by a line of cumulonimbus. *J. Atmos. Sci.,* **40,** 1815–1834.

——, and E. J. Zipser, 1980: Cumulonimbus vertical velocity events in GATE. Part I: Diameter, intensity and mass flux. *J. Atmos. Sci.,* **37,** 2444–2457.

Lenschow, D. H., and W. T. Pennell, 1974: On the measurement of in-cloud and wet-bulb temperatures from an aircraft. *Mon. Wea. Rev.,* **102,** 447–454.

Malkus, J. S., 1954: Some results of a trade-cumulus cloud investigation. *J. Meteor.,* **11,** 220–237.

Mazin, I. P., and S. M. Shmeter, 1977: Cumulus clouds and deformation of meteorological elements. *Trud. CAO,* **134**.

Musil, D. J., A. J. Heymsfield, and P. L. Smith, 1986: Microphysical characteristics of well-developed weak echo region in a High Plains supercell thunderstorm. *J. Climate Appl. Meteor.,* **25,** 1037–1051.

Nelson, L. D., 1982: Theory, electro-optical design, testing and calibration of a prototype atmospheric supersaturation, humidity and temperature sensor. U.S. Air Force Geophysics Laboratory Final Rep. AFGL-TR-32-0283, 107 pp.

Nicholls, S., E. L. Simmons, N. C. Atkinson, and S. D. Rudman, 1988: A comparison of radiometric and immersion temperature measurements in water clouds. Preprints, *10th Int. Conf. on Cloud Physics*, Hamburg, Germany, Amer. Meteor. Soc., 322–324.

Paluch, I. R., 1979: The entrainment mechanism in Colorado cumuli. *J. Atmos. Sci.,* **36,** 2467–2478.

——, and D. W. Breed, 1984: A continental storm with a steady, adiabatic updraft and high concentrations of small ice particles: 6 July 1976 case study. *J. Atmos. Sci.,* **41,** 1651–1664.

Pinus, N. Z., 1953: On aircraft measurements of air temperature in clouds. *Tr. Inst. CAO,* **12,** 13–17.

Rodi, A. R., and P. Spyers-Duran, 1972: Analysis of time response of airborne temperature sensors. *J. Appl. Meteor.,* **11,** 554–556.

Schemenauer, R. S., and G. A. Isaac, 1984: The importance of cloud top lifetime in the description of natural cloud characteristics. *J. Climate Appl. Meteor.,* **23,** 267–279.

Simpson, J., R. F. Adler, and G. R. North, 1988: A proposed Tropical Rainfall Measuring Mission (TRMM) satellite. *Bull. Amer. Meteor. Soc.,* **69,** 278–295.

Sinkevich, A. A., 1979: Application of IR-radiometer for thermal cloud characteristics measurements. *Tr. Inst. MGO,* **420,** 105–112.

——, 1981: The analysis of IR-radiometer operation in measuring temperature of clear-air and cloudy atmospheres. *Tr. Inst. MGO,* **439,** 93–102.

——, 1984: Investigation of the thermal characteristics of Cumulus Congestus using an IR Radiometer. *Meteor. Hydrol.,* **1,** 40–46.

——, 2001: *Cumulus Clouds of Northwest Russia*. Hydrometeoizdat, 106 pp.

Telford, J. W., and J. Warner, 1962: On the measurement from an aircraft of buoyancy and vertical air velocity in cloud. *J. Atmos. Sci.,* **19,** 415–423.

Wei, D., A. M. Blyth, and D. J. Raymond, 1998: Buoyancy of convective clouds in TOGA COARE. *J. Atmos. Sci.,* **55,** 3381–3391.

Zaytcev, V. A., and A. A. Ledohovich, 1970: *Devices for Cloud Investigations and Humidity Measurements*. Gidrometeoizdat, 256 pp.

Zvonarev, V. V., and A. A. Sinkevich, 1991: Aircraft methods of air temperature measurements in clouds. *Tr. Inst. MGO,* **543,** 24–33.